POST-PROCESS MACHINING OF ADDITIVE MANUFACTURED STAINLESS STEEL

Brandon M. Lane, Shawn P. Moylan, and Eric P. Whitenton
Intelligent Systems Division
Engineering Laboratory
National Institute of Standards and Technology
Gaithersburg, Maryland, USA

INTRODUCTION

Due to the poorer surface finish and geometric accuracy of additive manufactured (AM) parts compared to machined parts, it is inevitable that parts fabricated through AM processes will require post-process machining. This problem was identified early by machine manufacturers that make hybrid additive-subtractive systems. Apart from these complex systems, many AM part designs will require drilling, tapping, and surface finishing to meet their specified geometric tolerances, to satisfy the required functionality, or fit in an assembly.

There is already a substantial amount of research attempting to analyze, measure, model, and predict material microstructure and mechanical properties of AM materials [1]. However, the rapid growth of the AM industry and incorporation into the manufacturing landscape ensures the use of post-process or hybrid machining will outpace fundamental research and broad scientific understanding. However, some basic experiments can shed light on the potential challenges and pitfalls of post-process or in-process hybrid machining of AM materials. Machine shop personnel at the National Institute of Standards and Technology (NIST) have anecdotally reported more difficulty in milling, drilling, and tapping AM materials compared to their cast or wrought equivalent. This initiated an exploratory study into the machining characteristics of AM materials.

EXPERIMENT SETUP

AM disk specimens were fabricated in a laser powder bed fusion (PBF) machine using GP1 stainless steel powder (chemically equivalent to 17-4 stainless steel) with standard AM build parameters recommended by the machine manufacturer for this material. These parameters include two contour passes (laser exposures on the periphery of each build layer) before and after the internal areas are exposed: a pre-contour pass and post-contour pass respectively. These contour scans are conducted with a laser beam offset of 0.08 mm, laser power of 80 W, and scan velocity of 700 mm/s.

In conjunction, disks with similar geometry and 4.65 mm thickness were cut from wrought 17-4 stainless steel billet as baseline comparison. The AM disks were built on AISI 1045 steel build plates without support structure (directly fused to the build plates). Both AM disks (still attached to base plate) and baseline disks were put through a stress relief at 650 °C for 1 hour in Argon and allowed to air cool. The AM disks were separated from the build plates via wire electrical discharge machining (EDM), resulting in a thickness of 4.24 mm.

The periphery of the AM disks retained the sintered, powdery texture evident on all laser PBF parts. Both sets of disks were cut on the NIST orthogonal machining test center using the same instrumentation used in previous machining research at NIST [2]. Titanium-alumina-nitride (TiAlN) coated carbide grooving inserts were used to cut the disks. These had nominally 45 µm edge radius, 5° rake angle, and 6° clearance angle.

Six total tests were conducted; two on the baseline material and four on the AM material. Table 1 gives the machining conditions for these tests. Further cuts on the baseline material were not pursued after two cuts since forces achieved relatively consistent steady state and were considered exemplary for those cutting conditions. Cuts on the AM disk increased feed-rate after the initial two cuts. Thickness of the disk workpiece was 4.65 mm for the baseline and 4.24 mm for the AM disks. The difference in thickness of the AM and baseline disk is accounted for in the force analysis by reporting force values per disk thickness. At the end of each cut, the tool held position for 1.5 revolutions to clean up any radial runout in the disk which occurs if the tool is retracted quickly. Spindle speed was increased in each test from 167 rev/min for Test 1 to 171 rev/min for Test 6 to maintain constant surface speed while the disk diameter is reduced by cutting.

Table 1. Test order and machining parameters. All tests used the same tool.

Workpiece		Machine Input		
Test Name	Material	Surface Speed (m/min)	Feed Rate (mm/rev)	Cut Surf. Distance (m)
Test 1	Wrought	60.00	0.070	1.500
Test 2	Wrought	60.00	0.070	1.500
Test 3	AM	60.00	0.070	1.500
Test 4	AM	60.00	0.070	1.500
Test 5	AM	60.00	0.140	1.500
Test 6	AM	60.00	0.280	1.500

A high speed visible light camera with macro lens was positioned normal to the tool rake face and captured video of chip formation at 4000 frames/s (a period of 0.25 ms/frame). In addition, a 3 axis dynamometer captured machining forces in the cutting, normal, and side directions at 1 MHz. Figure 1 shows the placement of the tool holder, camera, and workpiece in the machining test center. The AM disk was positioned on the spindle such that the EDM surface, which coincides with the bottom of the build during laser PBF fabrication, faces the front of the machine (viewed by the operator), and faces the right-hand side in the high speed videos.

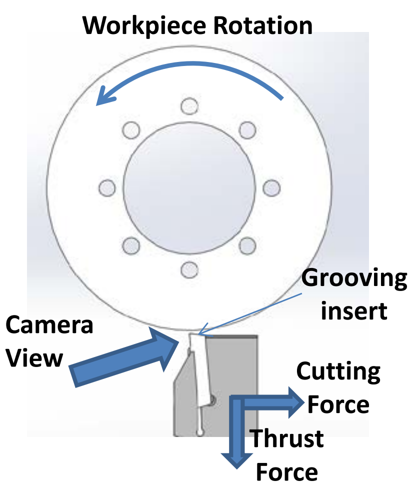

Figure 1. Schematic of workpiece rotation, tool and camera position. AM build direction is into the screen.

FORCE RESULTS

Figure 2 gives three example force plots from three tests. These show 1 MHz force data downsampled to 1 kHz. Mean side tool forces directed out of the machining plane were below 2.5 N/mm and are not visible in Figure 2.

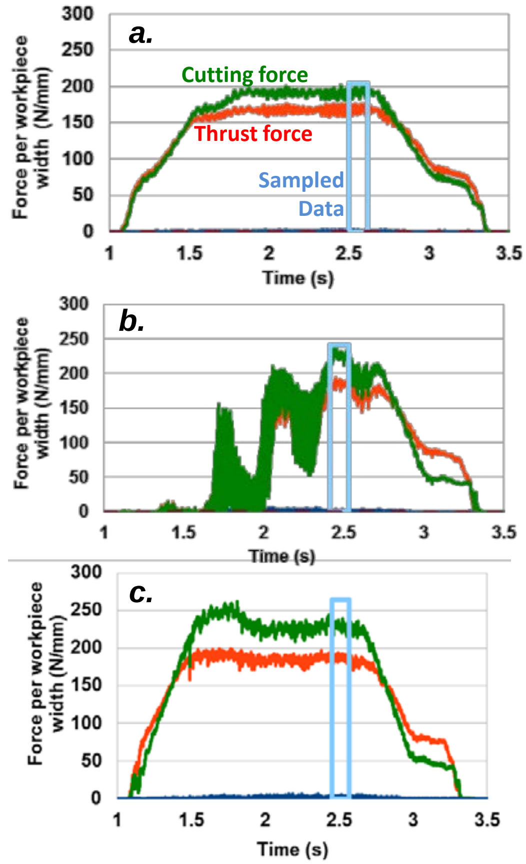

Figure 2. a. Test 2 (wrought material) showed relatively stable cutting which achieved steady state after one rotation. b. Test 3 (first cut on AM disk) showed noisy unsteady forces resulting from rough surface and radial runout. c. Test 4 (second cut on AM disk) showed stable cutting similar to wrought material, but noticeably higher cutting and thrust forces.

Table 2 gives summary statistics of the collected forces for the ‘Sampled Data’ regions shown in Figure 2. ‘Mean Tool Forces’ are defined as the mean of the 1 kHz data downsampled taken over 0.3 disk revolutions at a time subjectively chosen to be near ‘steady state’ forces. The standard deviation was calculated for every 1 000 sample bin from the 1 MHz data, and the mean of this standard deviation data is defined in the ‘Vibration’ columns in Table 2. This gives a measure of force vibrations above 1 kHz.

Table 2. Summary of force statistics taken from 'sampled data region' consisting of 0.3 disk revolutions. Test 1 forces were not acquired due to faulty equipment triggering.

Test Name	Mean Tool Forces 1 kHz downsampled Side (N/mm)	Thrust (N/mm)	Cutting (N/mm)	Vibration Mean of 1000-pt. std. dev. Side (N/mm)	Thrust (N/mm)	Cutting (N/mm)
Test 1	-	-	-	-	-	-
Test 2	0.56	168.44	191.72	8.42	10.03	14.85
Test 3	1.02	183.57	225.68	13.72	20.63	27.09
Test 4	1.31	187.73	229.01	23.32	25.38	36.10
Test 5	2.42	221.73	371.97	26.40	39.51	65.56
Test 6	1.87	255.06	589.92	45.92	60.95	147.3

For the same cutting conditions, the per width thrust and per width cutting forces were approximately 11% and 19% higher, respectively for AM materials in Test 4 vs. Test 2. AM disks cause much more high frequency noise. As seen in Figure 2b, the first cut on the AM disk (Test 3) did not achieve a steady state, therefore the force statistics are not comparable to the wrought material.

HIGH SPEED VIDEO OBSERVATIONS

Tests 1 and 2 on the wrought material did not show any notable phenomena. Continuous chips formed immediately after the tool contacted the workpiece, as shown in Figure 3. Smoke can be seen stemming from the cutting region, likely due to heating of residual machining oils on the tool or workpiece. One of the fiber illumination sources was placed behind the tool towards the right in the movie frames, also seen in Figure 3. Videos for Test 4 through Test 6 on the AM material did not show any significant observations either. Chips were continuous from the beginning to end of cutting. Segmentation on the back of the chips was clearly visible in Test 5 and 6, with the segments being larger for Test 6. These segments, which increased from test 4 to 6 along with the feed rate, typically coincide with adiabatic shear banding, though also depend on cutting speed, tool rake angle, and coolant/lubrication [3].

Table 3 outlines the timing of observable phenomena of interest seen in Test 3, which was the first cut on the AM material. Chip formation on this material started with powdery debris and dislocated chips; transition into continuous chips which curled sharply to the right of the frame with visible, periodic dark striations on the back of the chip; then transitioned into normal chip curl.

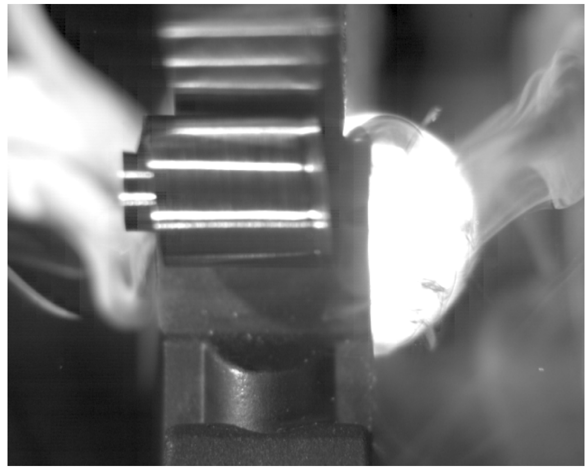

Figure 3. Test 1 showed continuous chips which curled nominally in the orthogonal cutting plane.

Table 3. Phenomena observed in Test 3 high speed video and their relative time of occurrences.

Frame	Time (ms)	Spindle Revs (revs)	Total Feed (mm)	Observations
1400	0	0	0	Tool contacts workpiece.
-	-	-	-	Chips are powdery and dislocated.
2784	346.0	0.97	0.068	Continuous chip formation starts. Chips show tight curl with dark striations.
-	-	-	-	Continuous chips with striations
5430	1007.5	2.84	0.199	Striations disappear. Chip curl is less severe.
6522	1280.5	3.61	0.252	Tool stops feeding into workpiece.
-	-	-	-	Chip becomes thinner as effective depth of cut is reduced.
7662	1565.5	4.41	0.309	Chip formation stops

Variation in chip curl

Normally, during orthogonal cutting of wrought materials, chip curl occurs in the same plane as the cutting direction and workpiece rotation, as was observed in Tests 1 and 2 and shown in Figure 3. However, after continuous chips started forming in Test 3, these chips curled sharply to the right as seen in Figure 4b. After further cutting, the sideways chip curl subsided.

In laser PBF and other laser-based AM processes, residual stresses occur in the part after it is formed and cooled. Some stresses may still exist even after a stress relief heat treat cycle, as was done with the AM parts in this study. These residual stresses depend on the material, part geometry, laser scan strategy, and multiple other factors. Generally, the top of the AM build forms tensile stresses, while the interior or bottom are compressive [4,5]. With regard to the sideways chip curl seen in Figure 4b, this may be a result of the release of tensile stresses on the left side of the chip, which coincides with the top of the AM build. It is theorized that plastic deformation of the chip causes the residual negative strain to normalize, which effectively causes expansion which pushes the chip to the side. As the tool cuts further and enters the interior of the part, the residual stresses may be lower, therefore resulting in reduced side bending of the chip seen in Figure 4c and in later Tests 5 and 6.

Striations on the back of the chip

As mentioned in the observations in Table 3 and evident in Figure 4b, periodically formed dark striations could be seen on the back of the chip in Test 3. Prior to the machining tests, the inner diameter of the AM workpiece disk was lathe turned in order to fit on the machining center spindle. These striations were also evident on the resulting interior surface, as shown in Figure 5a-b. The spacing of the striations (approximately 5 mm) coincided with the spacing of triangular faces formed when the solid part file is converted to a stereo-lithography (STL) file. This also results in slightly visible faceting on the periphery of the uncut AM disk, which causes high and low spots on the surface, and varies the effective depth of cut. However, striations were apparent over more than one disk revolution, and appeared up to 0.20 mm total feed. This is much larger than the effective high/low spots on the periphery of the disk with 5 mm facets, and indicates that the striation features are formed or exist further into the interior of the disk at a distance affected by the contour exposure during the laser PBF build.

CONCLUSIONS

These machining tests were originally designed to make subjective observations, and guide development of future, more scientifically rigorous tests. Based on these results, two phenomena are of further interest: chip curl due to surface residual stresses and surface features due to part file tessellation. The following conclusions are made:

- Mean cutting and thrust forces and high frequency vibration were higher for the AM material.
- Chip curl on the AM material is likely affected by residual stress. The chip is pushed away from regions of tensile stress released after plastic deformation.
- Tesselated surfaces of the STL part file is a likely cause of the observed chip surface striations. However, the striations appear at cut depths deeper than the effective high/low spots caused by faceted perimeter of the disk.

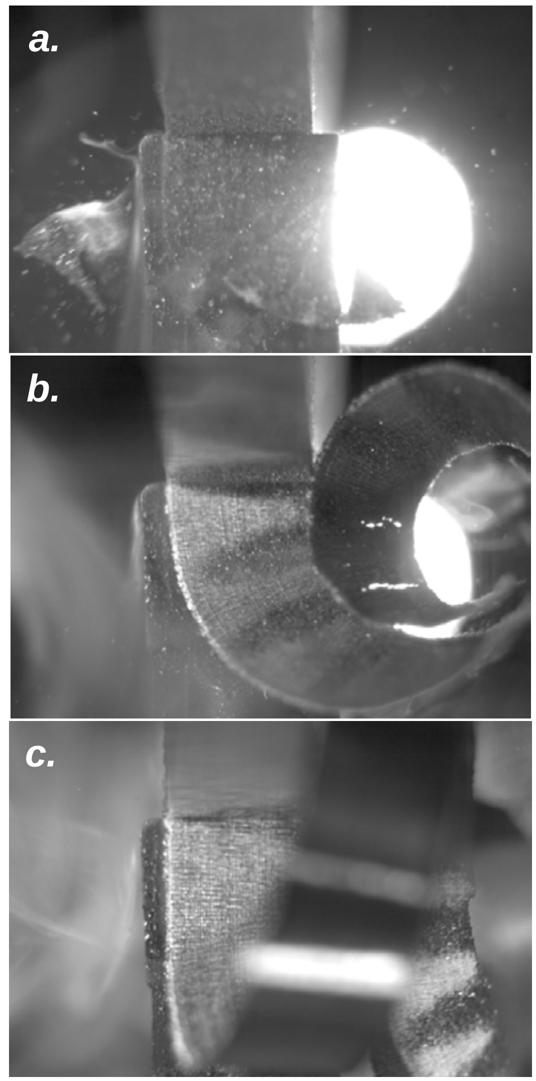

Figure 4. a. Test 3 frame 1920 shows powdery, dislocated chips and debris. b. Frame 3176 shows continuous chips which curl sharply to the right and have dark striations on the back. c. Frame 5634 shows continuous chips with less severe chip curl. The shiny, new cut surface is closer to the camera and out of focus. Striations can be seen further to the right on the previously formed chip surface.

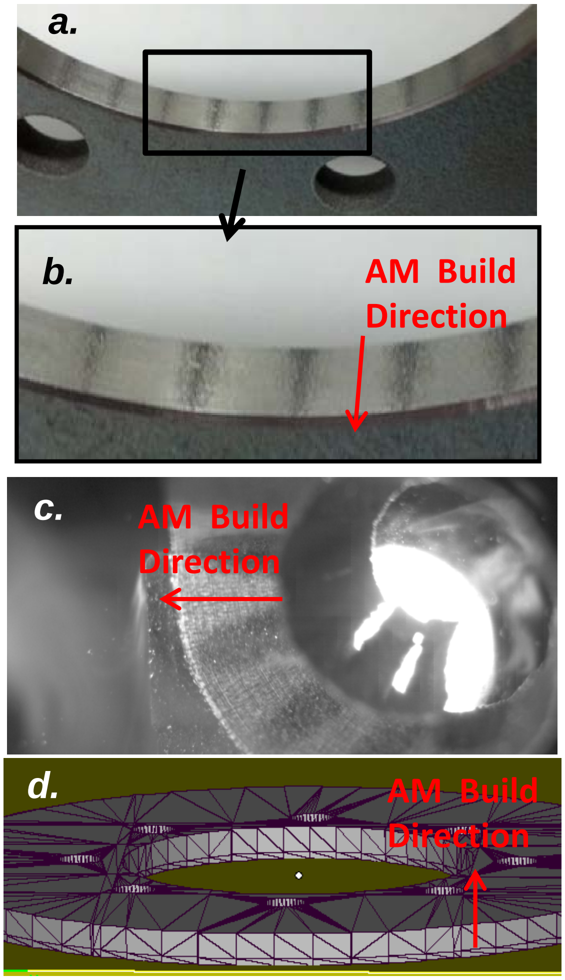

Figure 5. a. Lathe turned inner diameter of the workpiece showing light/dark striations. b. Enhanced view of striations on the workpiece. c. Striations appearing on the chip surface in high speed video (Test 3, frame 3154) and the relation to the build direction. d. STEP file of disk showing tesselated facets on the inner and outer periphery.

FUTURE WORK

Since near net-shape parts are possible with AM, it is presumed that only relatively shallow or finish machining would be of interest and the main objective being to optimize surface form and finish. It is presumed that manufacturers will not push tool life requirements for AM part machining and will absorb the added cost of potentially switching tools prematurely. This is due to the fact that AM parts have already accumulated high value based on the design and AM build times prior to any post-process machining, and tool cost is relatively low compared to the risk of scrapping an AM built part. However, tool breakage could be a potentially large cost factor for machined AM parts if they must be scrapped. Therefore, continued research on machining of AM materials should detail tool wear and tool forces. Apart from this, further machining experiments on AM materials conducted at NIST will focus on two phenomena based on the results of this preliminary study.

Chip formation vs. laser PBF contour scanning strategy

As previously mentioned, residual stresses in laser PBF parts are affected by multiple factors. Two factors; laser scan strategy and heat treatment, are candidate variables that manufacturers may choose to enable better conditions for post-process machining. It was observed in this study that the stress-affected chip curl mostly occurs closer to the part surface at depths primarily created during the pre- and post-contour scanning during the AM build. Further studies will attempt to observe how the chip curl is affected by different contour scan strategies. If residual stress release is a dominant factor in chip curl, then this may have an ultimate effect on surface form as well. Varying stress relief heat treat cycle, or observing the chip characteristics on fully annealed samples will also galvanize the idea that chip curl is largely affected by chip curl, and guide manufacturers towards an optimized heat treatment.

In addition, multiple methods and standards exist for stress measurement by material removal [4]. New methods for observing and quantifying residual stress by machining may be possible.

Surface finish vs. STL surface tessellation

Though surface finish of the disks was not measured in this preliminary study, the striations seen on the chip and machined surface in Figure 5 form an obvious periodic change in surface finish. Since one purpose for machining AM parts is to improve surface finish, mitigating these striations is important. Varying the STEP file tessellation on machined parts may further elucidate the cause of the striations, and surface finish measurement will quantify their effect on overall surface finish. Another important factor is how deep into the workpiece material the striations appear and affect the surface, that is, how much material must be removed to negate their effect. Smaller feeds than those used in this study may better resolve the total cutting depth at which the striations disappear. Results from this study will create part design rules if post-process machining for improved surface finish is necessary.

REFERENCES

[1] Mani M, Lane B, Alkan MA, Feng S, Moylan S, Fesperman R. Measurement science needs for real-time control of additive manufacturing powder bed fusion processes NISTIR 8036. Gaithersburg, MD: National Institute of Standards and Technology; 2015.

[2] Madhavan V, Lipczynski G, Lane B, Whitenton E. Fiber orientation angle effects in machining of unidirectional CFRP laminated composites. J Manuf Process n.d.;In Press - Corrected Proof. doi:10.1016/j.jmapro.2014.06.001.

[3] Deshayes L, Mabrouki T, Ivester R, Rigal J-F. Serrated chip morphology and comparison with finite element simulations. Proc. IMECE04, Anaheim, CA: American Society of Mechanical Engineers; 2004, p. 815–24.

[4] Kruth J-P, Deckers J, Yasa E, Wauthlé R. Assessing and comparing influencing factors of residual stresses in selective laser melting using a novel analysis method. Proc Inst Mech Eng Part B J Eng Manuf 2012;226:980–91. doi:10.1177/0954405412437085.

[5] Gnäupel-Herold T, Slotwinski J, Moylan S. Neutron measurements of stresses in a test artifact produced by laser-based additive manufacturing. AIP Conf. Proc., vol. 1581, Baltimore, MD: AIP Publishing; 2014, p. 1205–12.

 The full descriptions of the procedures used in this paper require the identification of certain commercial products. The inclusion of such information should in no way be construed as indicating that such products are endorsed by NIST or are recommended by NIST or that they are necessarily the best materials, instruments, software or suppliers for the purposes described.